



## Short communication

Antiglare and antireflective coating of layer-by-layer SiO<sub>2</sub> and TiZrO<sub>2</sub> on surface-modified glassChairul Hudaya<sup>a</sup>, Bup Ju Jeon<sup>b,\*</sup>, Ariono Verdianto<sup>a</sup>, Joong Kee Lee<sup>c,d</sup>, Yung-Eun Sung<sup>e,f,\*\*</sup><sup>a</sup> Electric Power and Energy Materials (EMAT), Department of Electrical Engineering, Faculty of Engineering, Universitas Indonesia, Kampus Baru UI, Depok 16424, Indonesia<sup>b</sup> Department of Energy and Environmental Engineering, Shinhan University, Dongducheon 11340, Republic of Korea<sup>c</sup> Center for Energy Storage, Green City Technology Institute, Korea Institute of Science and Technology, Seoul 02792, Republic of Korea<sup>d</sup> Department of Energy and Environmental Engineering, KIST School, Korea University of Science and Technology, Seoul 02792, Republic of Korea<sup>e</sup> Center for Nanoparticle Research, Institute for Basic Science (IBS), Seoul 08826, Republic of Korea<sup>f</sup> School of Chemical and Biological Engineering, Seoul National University, Seoul 08826, Republic of Korea

## ARTICLE INFO

## Keywords:

Antiglare  
Antireflection  
Layer-by-layer coating  
Transparent optical materials  
SiO<sub>2</sub>  
TiZrO<sub>2</sub>

## ABSTRACT

Antiglare and antireflection materials take considerable research attention due to its important role in transparent optical materials for various purposes. In this study, we employed layer-by-layer coating materials consist of SiO<sub>2</sub> and TiZrO<sub>2</sub> deposited on etched-surface glass substrate using dual electron beam evaporator system. The surface morphology investigated by using scanning electron microscopy (SEM) exhibited the microstructure patterns of glass surface. The cross-sectional image of transmission electron microscopy (TEM) showed uniformly layer-by-layer coating materials with the thickness of ~20–80 nm. The Auger electron spectroscopy (AES) revealed the depth profiles of elemental composition of surface layer-by-layer coating, confirming the presence of elements of SiO<sub>2</sub> and TiZrO<sub>2</sub> layers. In addition, the layer-by-layer coated glass surface performed the hydrophobic properties with contact angle of 69°. The microstructure surface treatment and layer-by-layer coating have successfully decreased the reflectance (~3%) and increased the transmittance of the treated glass (~91%), opening the possibility for the applications of any optical devices.

## 1. Introduction

In the major transparent optical materials, the cover glass of photovoltaic (PV) cells which generally composed of silica (SiO<sub>2</sub>) reflects about 4.3% of the incident visible light with refractive index of ~1.5 [1]. Huge market demands for optoelectronic and optical in diverse area has triggered the urgency to seek out the alternative option improving the performance of this material for certain purposes. For instance, suppressing the light reflection would contribute a beneficial impact in increasing the efficiency of optical materials, including photovoltaic panels, laser-related devices, optical lenses and display devices [2,3]. A lot of research groups have been intensively working on the development of antiglare and antireflective coating on glass using layer-by-layer coatings and nanostructured patterning [4]. Light reflection employing a layer-by-layer coated surface can be decreased into a certain degree through modification of the light interference at different coating layers. Nevertheless, the light reflection often occurs only within the range of visible wavelength [5].

SiO<sub>2</sub> is highly preferable transparent coating materials for the PV cells since its excellent transparency and easy preparation [6,7]. The efficiency of PV module performance could be improved by optimizing the capture of the incident light through antireflective glass [8]. Furthermore, it has been demonstrated that SiO<sub>2</sub> has the efficiency of antireflective properties, good scratch resistance, low refractive index and chemical stability on the glass substrate [9,10].

Considering mechanical strength and biocompatibility, TiZrO<sub>2</sub> composite has widely catch the attention in medical and aerospace application [11]. Stress-induced transformation of ZrO<sub>2</sub> crystal framework can be used in intensifying fracture toughness of a material [12,13]. In this study, we developed the novel concept of layer-by-layer coating materials made of SiO<sub>2</sub> and TiZrO<sub>2</sub> on the surface-modified glass for any transparent optical materials. It was believed that this material enabled the decrease of reflectance and enhancement of light transmittance. Furthermore, it exhibited the hydrophobic properties, allowing the possibility for the application in solar panel and any other transparent conducting materials that need the combination of

\* Corresponding author.

\*\* Correspondence to: Y.-E. Sung, Center for Nanoparticle Research, Institute for Basic Science (IBS), Seoul 08826, Republic of Korea.

E-mail addresses: [bjjeon@shinhan.ac.kr](mailto:bjjeon@shinhan.ac.kr) (B.J. Jeon), [ysung@snu.ac.kr](mailto:ysung@snu.ac.kr) (Y.-E. Sung).

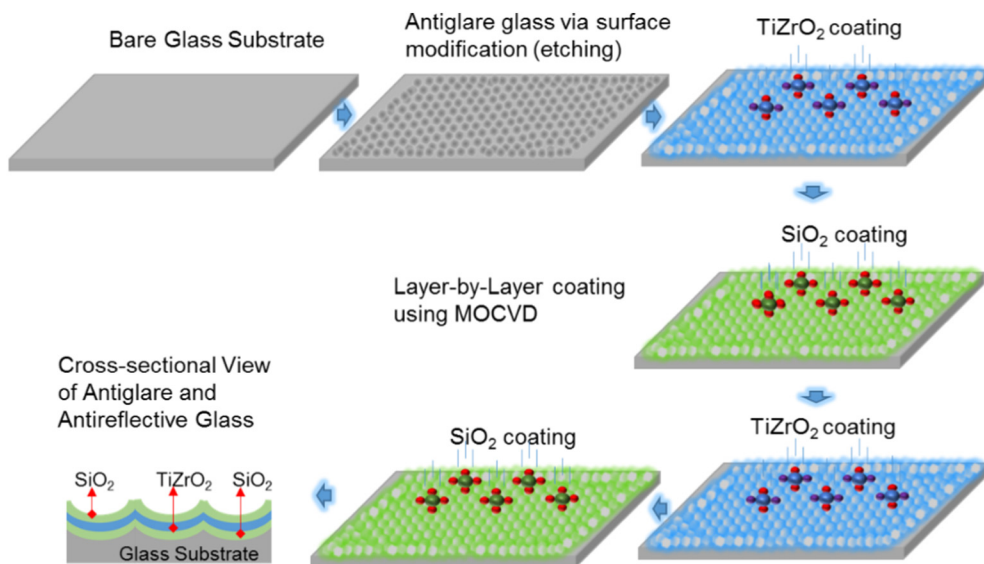


**Fig. 1.** The preparation of antiglare and antireflection thin-film coating on surface-treated glass including the etching process using acidic solution and homogeneous thin film coating on surface-treated glass using dual electron beam evaporator system.

antiglare and antireflection features.

## 2. Materials and methods

### 2.1. Preparation of antiglare and antireflection glass

The schematic diagram of experimental works in this study to design the layer-by-layer thin film coating is represented in Fig. 1. In regard the surface substrate modification, the chemical etching agent  $\text{NH}_4\text{F}_2$ , was used to change the structure of relatively flat substrate surface into a rugged one. Then, subsequent deposition of  $\text{SiO}_2$  and  $\text{TiZrO}_2$  using dual beam electron beam evaporator system was carried out under the base pressure of  $4 \times 10^{-5}$  Torr. The experimental details were provided in Supplementary Material.

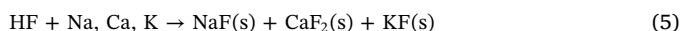
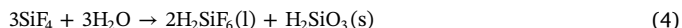
### 2.2. Materials characterizations

The materials characterizations were performed through Scanning Electron Microscopy (SEM, Hitachi S-3400 FE-SEM) to identify the surface morphology, Transmission Electron Microscopy (TEM, Tecnai FEI) to reveal the cross-sectional image of the materials, in which the sample was previously prepared by a Focus Ion Beam (FIB-Nova), Energy-Dispersive X-ray spectroscopy (EDX, TEM Tecnai FEI), Auger Electron Spectroscopy (AES, ULVAC-PHI 700) to find the materials composition in the depth profile, ultraviolet-visible spectroscopy (UV-Vis, Varian 5000) to reveal the reflectance, transmittance and reflectance of the light and contact angle measurement to find the angle

of hydrophobicity of materials for the bare glass, antiglare glass (AG) and antiglare-antireflection coated glass substrate (AG/AR).

## 3. Results and discussion

During the surface etching, the reaction between the glass, water and solution performs the following equations:



Briefly, the simplest engraving agent for etching or frosting glass is hydrofluoric acid which can be formed by reacting ammonium difluoride and water molecule. If this strong acid is released contacting with the glass surface, the glass will be dispersed until all the hydrofluoric acid has been transformed into hydrofluosilicic acid. Another possible product of the reaction between hydrofluoric acid and silica is a colorless gas silicon tetrafluoride. This gas rapidly hydrolyzed by water forming hydrated silica and fluorosilicic acid. The entire process will not have affected the transparency of the glass then it will allow the light passing through [14].

The surface morphology the bare glass shows a typical flat surface morphology (Fig. 2a), meanwhile for surface-treated antiglare glass, it

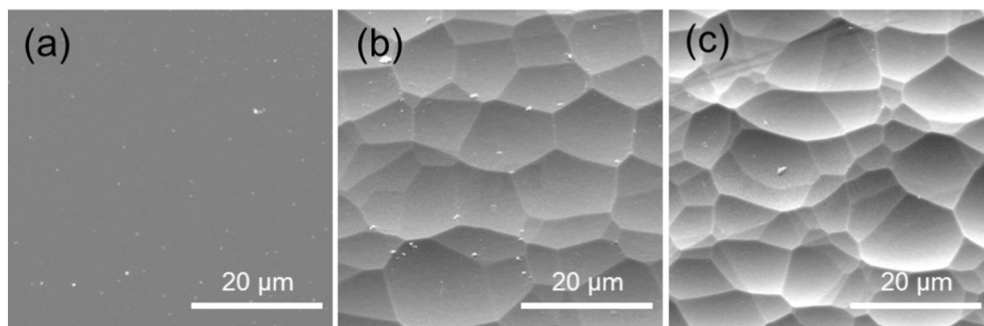


**Fig. 2.** Scanning electron microscopy (SEM) images of (a) bare glass, (b) surface-etched antiglare glass and (c) antiglare-antireflection coating glass.

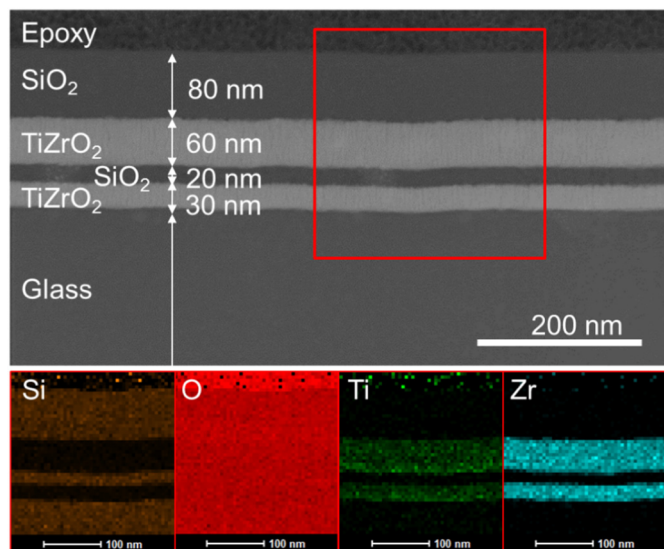


Fig. 3. Cross-sectional HR-TEM images of layer-by-layer  $\text{SiO}_2$ - $\text{TiZrO}_2$ -coated surface-etched glass.

exhibited the microstructure-pattern due to the reaction during the etching process (Fig. 2b). It is hard to distinguish directly from the SEM images the difference between surface-etched antiglare glass (Fig. 2b) and antiglare-antireflective coating glass (Fig. 2c) which obviously due to the nanoscale thickness of thin film, making it identical surface architecture.

TEM and EDX analysis were performed to examine the surface structure of the prepared-substrate and its component (Fig. 3). TEM images show the cross-sectional area representing the sandwich of layer-by-layer  $\text{SiO}_2$ - $\text{TiZrO}_2$  on the surface-etched glass and the thickness of each layer as well. In the outer layer, 80 nm-thick  $\text{SiO}_2$  layer was successfully deposited, followed by 60 nm-thick of  $\text{TiZrO}_2$ , 20 nm-thick of  $\text{SiO}_2$  and 30 nm-thick  $\text{TiZrO}_2$ . These optimized layers were expected to enhance light transmission and at the same time reduce light reflection. The elemental scanning data confirmed the present of Si, O, Ti and Zr compositions and it shows well-dispersed and solid uniformity distribution of coating materials on the substrate surface.

Fig. 4 represents the AES depth profile analysis data to further disclose the properties of coating materials. We collected depth elemental data at 5 different-spotted areas according to its depth and it is firmly confirmed the existence of Si, Ti, Zr and O elements. The inclusion of Ca was suspected come from the glass substrate as previously

explained in surface reaction equations.

The optical properties of the glass in regard the transmission and reflection of incoming light has been inspected by using UV-Vis spectroscopy (Fig. 5a). It can be inferred that the layer-by-layer coating of  $\text{SiO}_2$  and  $\text{TiZrO}_2$  on the microstructure glass substrate has decreased the reflectance  $\sim 3\%$  of light reflection, from approximately 6% at the normal incidence ray and center specific wavelength ( $\sim 400\text{ nm}$ – $800\text{ nm}$ ) for the bare and etched-surface glass. It is interesting to note that the coating materials enable the suppression transmittance within the near-infrared zones, making it to have the selective ability in preventing undesired light for being transmitted. The refractive index and extinction coefficient of the samples were calculated (Fig. 5b). The etching process slightly effected the optical properties of the substrate which obviously can be seen through slightly lower the refractive index. The surface modification of substrate by layer-by-layer coating has significantly decreased the optical properties of the sample that is indicated by the refractive index of 1.31. However, the level of surface roughness plays a big role in determining the optical constant of the substrate. Moreover, absorption of the electromagnetic wave energy during its travelling in a medium or material was characterized by extinction coefficient of the thin film. The estimated extinction coefficients of the observed samples are 0.0131, 0.0352, and 0.0142, for bare, AG and AG/AR glass, respectively (refers to Supplementary material (S1)). The deposition of the coating material onto the surface-modified glass substrate was not significantly altered the extinction coefficient of the substrate from the initial condition.

To get a better understanding of the hydrophobic properties of the glass surface, the contact angle of the water droplets was evaluated (Fig. 6). The hydrophobicity of a surface was believed associated with the self-cleaning capability and self-detaching any dust from the surface of the coated glass which favorably in some applications such as for PV panels [15,16]. The contact angle of AG/AR glass has the highest value of  $69^\circ$  among those glasses, closed to  $90^\circ$  minimum hydrophobic identity, surpassing the bare glass and AG glass, each was  $27.5^\circ$  and  $59.7^\circ$ , respectively. Another possible explanation for this discover is the surface chemical modification and coating material deposition affected the surface free energy [17]. The decreasing contact angle describes that the water droplets are favorable to adhere to the uncoated-surface which is obviously identified in the SEM images (Fig. 2a). Thus, here the surface roughness and thin film layer-by-layer coating play significant roles to the resulting water contact angle.

Giving a demonstration correlated to the reflection phenomenon of a glass, we took a photograph of three types of glass (Fig. 7). We observe that the text on the screen was reflected onto the surface of the bare glass. Meanwhile, this could not be found on the AG and AG/AR

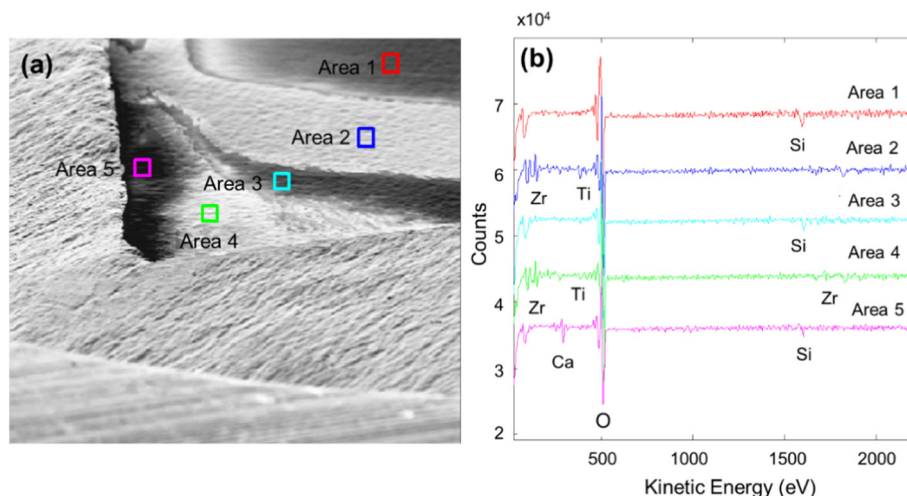
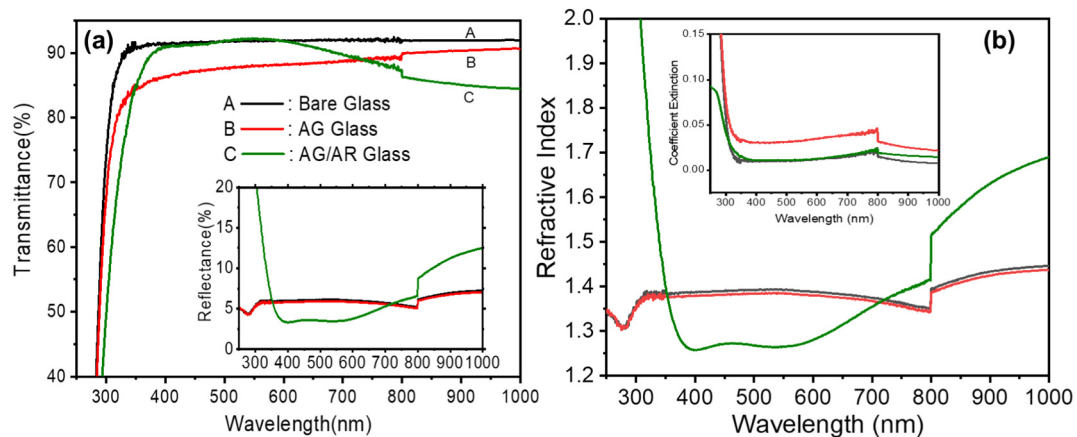
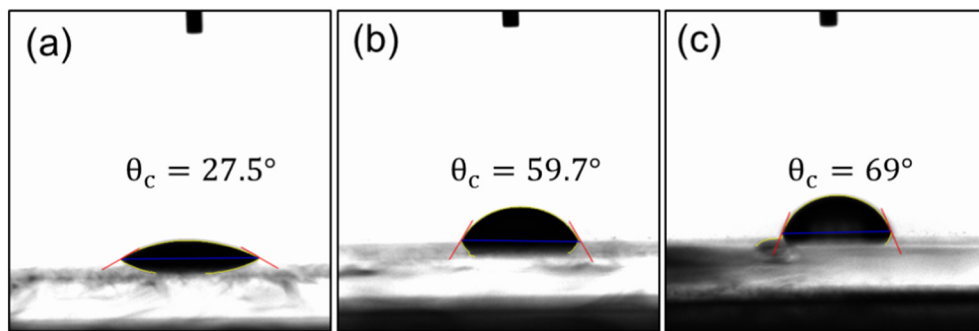


Fig. 4. Auger Electron Spectroscopy (AES) (a) photograph of depth profile (b) elemental composition of  $\text{SiO}_2$ - $\text{TiZrO}_2$ -coated surface-etched glass.



**Fig. 5.** (a) Transmittance and reflectance (inset) spectra; (b) refractive index and coefficient extinction (inset) plot are measured in a visible and near-infrared wavelength of (A) bare glass, (B) surface-etched antiglare glass and (C) antiglare-antireflective coating glass.



**Fig. 6.** Contact angle of (a) bare glass, (b) surface-etched glass and (c) layer-by-layer  $\text{SiO}_2\text{-TiZrO}_2$ -coated surface-etched glass.



**Fig. 7.** Photograph of (a) bare glass, (b) AG glass and (c) AG/AR glass.

glass surface. Furthermore, the AG/AR glass shows higher transparency than that of the AG glass. This phenomenon is in good agreement with the result of UV–Vis spectroscopy.

#### 4. Conclusion

A novel layer-by-layer antiglare and antireflective coating made of  $\text{SiO}_2\text{-TiZrO}_2$  thin film has been prepared on the surface-etched glass for transparent optical materials. The coating materials were homogeneously coated on the surface microstructure pattern of the glass using dual beam electron evaporator technique. We found that the layer-by-layer thin film coating materials (20–80 nm) have enhanced

the transmittance (~91%) in visible wavelength (300–600 nm) and decreased it in the near-infrared zone (700–1000 nm). In addition, the AG/AR glass showed the hydrophobic properties, by increasing the contact angle from  $27.5^\circ$  to  $69^\circ$  after being treated with layer-by-layer deposition. These features open any possible applications requiring high transmittance, such as solar panel systems and any optical lenses.

#### Acknowledgment

C. H. was grateful with the support of 2018 Program Academic Recharging – World Class University (PAR-WCU) Universitas Indonesia, funded by Ministry of Research, Technology and Higher Education, Republic of Indonesia (Contract No. 263.2/D2.3/KP/2018). This study was also partially supported by KIST School Alumni Partnership Project and USAID through Sustainable Higher Education Research Alliances (SHERA) Project for Universitas Indonesia's SMART CITY Center for Collaborative Research. J.K.L. was grateful with research grants of NRF (NRF-2019R1A2B5B03001772) funded by the National Research Foundation under the Ministry of Science and ICT, Republic of Korea and Korea Institutional Program (2E29592). Y.-E. S. acknowledges that this work was support by the Institute for Basic Science (IBS) in Republic of Korea (Project Code: IBS-R006-D1).

#### Appendix A. Supplementary data

Supplementary data to this article can be found online at <https://doi.org/10.1016/j.apsusc.2019.06.027>.

#### References

- [1] B.G.S. Priyadarshini, A.K. Bull, Design of multi-layer anti-reflection coating for terrestrial solar panel glass, *Bull. Mater. Sci.* 39 (2015) (2016) 683–689.

- [2] C. Domínguez, I. Antón, G. Sala, Solar simulator for concentrator photovoltaic systems, *Opt. Express* 16 (2008) 14894–14901.
- [3] D. Das, A. Banerjee, Anti-reflection coatings for silicon solar cells from hydrogenated diamond like carbon, *Appl. Surf. Sci.* 345 (2015) 204–215.
- [4] J. Bico, C. Marzolin, D. Quéré, Pearl drops, *EPL (Europhysics Letters)* 47 (1999) 220.
- [5] S. Kim, U.T. Jung, S.-K. Kim, J.-H. Lee, H.S. Choi, C.-S. Kim, M.Y. Jeong, Nanostructured multifunctional surface with antireflective and antimicrobial characteristics, *ACS Appl. Mater. Interfaces* 7 (2015) 326–331.
- [6] Y. Gao, I. Gereige, A. Labban, D. Cha, T. Isimjan, P.M. Beaujuge, Highly Transparent and UV-resistant Superhydrophobic SiO<sub>2</sub>-coated ZnO Nanorod Arrays, (2014).
- [7] X. Deng, L. Mammen, Y. Zhao, P. Lellig, K. Müllen, C. Li, H.-J. Butt, D. Vollmer, Transparent, thermally stable and mechanically robust superhydrophobic surfaces made from porous silica capsules, *Adv. Mater.* 23 (2011) 2962–2965.
- [8] Y. Li, Y. Zhang, J. Lin, C. Fang, Y. Ke, H. Tao, W. Wang, X. Zhao, Z. Li, Z. Lin, Multiscale array antireflective coatings for improving efficiencies of solar cells, *Appl. Surf. Sci.* 462 (2018) 105–111.
- [9] M. Karpe, G. Mezinskis, Synthesis of Micro- and Mesoporous SiO<sub>2</sub> Based Ceramic Materials (Using Sol-gel Technology), (2014).
- [10] M. Mazur, D. Wojcieszak, D. Kaczmarek, J. Domaradzki, S. Song, D. Gibson, F. Placido, P. Mazur, M. Kalisz, A. Poniedzialek, Functional photocatalytically active and scratch resistant antireflective coating based on TiO<sub>2</sub> and SiO<sub>2</sub>, *Appl. Surf. Sci.* 380 (2016) 165–171.
- [11] H. Tsukamoto, Mechanical properties of zirconia-titanium composites, *International Journal of Materials Science and Applications* 3 (5) (2014) 260–267.
- [12] P.M. Kelly, L.R. Francis Rose, The martensitic transformation in ceramics — its role in transformation toughening, *Prog. Mater. Sci.* 47 (2002) 463–557.
- [13] H. Tsukamoto, Micromechanical modeling of transformation toughening in multi-phase composites enriched with zirconia particles, *Comput. Mater. Sci.* 48 (2010) 724–729.
- [14] W.S. Kahlson, Studies on the Etching of Glass1, (2006).
- [15] C. Zhou, Y. Li, H. Li, X. Zeng, P. Pi, X. Wen, S. Xu, J. Cheng, A self-cleaning titanium mesh with underwater superoleophobicity for oil/water separation and aqueous pollutant degradation, *Surf. Coat. Technol.* 313 (2017) 55–62.
- [16] H. Wang, Z. Liu, E. Wang, X. Zhang, R. Yuan, S. Wu, Y. Zhu, Facile preparation of superamphiphobic epoxy resin/modified poly(vinylidene fluoride)/fluorinated ethylene propylene composite coating with corrosion/wear-resistance, *Appl. Surf. Sci.* 357 (2015) 229–235.
- [17] J. Conti, J. De Coninck, M.N. Ghazzal, Design of water-repellant coating using dual scale size of hybrid silica nanoparticles on polymer surface, *Appl. Surf. Sci.* 436 (2018) 234–241.